Short communication

Synthesis of ordered mesoporous ruthenium by lyotropic liquid crystals and its electrochemical conversion to mesoporous ruthenium oxide with high surface area

Wataru Sugimoto [a,b,*], Sho Makino [a], Ryota Mukai [a], Yoshiaki Tatsumi [a], Katsutoshi Fukuda [b,1], Yoshio Takasu [a], Yusuke Yamauchi [c,d,**]

[a] Faculty of Textile Science and Technology, Shinshu University, 3-15-1 Tokida, Ueda, Nagano 386-8567, Japan
[b] Collaborative Innovation Center for Nanotech Fiber, Shinshu University, 3-15-1 Tokida, Ueda, Nagano 386-8567, Japan
[c] World Premier International Research Center for Materials Nanoarchitectonics, National Institute for Materials Science, Namiki 1-1, Tsukuba, Ibaraki 305-0044, Japan
[d] Precursory Research for Embryonic Science and Technology, Japan Science and Technology Agency, Kawaguchi, Saitama 332-0012, Japan

ABSTRACT

In ordered to prepare high capacitance pseudo-capacitive oxides, it is important to design nanostructures with appreciable mesopores. Supramolecular templating has become a popular method to synthesize ordered mesoporous metals; however, the application of the same technique to synthesis of high surface area oxides is more demanding. We present here, the synthesis of ordered mesoporous ruthenium metal by lyotropic liquid crystal templating and its electrochemical conversion to ordered mesoporous ruthenium oxide by a simple, room temperature procedure. The bulk, unsupported metallic ordered mesoporous ruthenium exhibits high surface area of $110 \, m^2 \, g^{-1}$, which is comparable to typical supported Ru nanoparticles. The oxide analogue gives a high specific capacitance of $376 \, F \, g^{-1}$, owing to the porous structure. These results demonstrate a possible facile and generic process to synthesize oxides with ordered nanostructures by utilization of the various phases that can be obtained with lyotropic liquid crystalline templates such as cubic, hexagonal, lamellar, etc.

© 2011 Elsevier B.V. All rights reserved.

1. Introduction

Since the pioneering work by Attard and co-workers [1,2], ordered mesoporous metals prepared by supramolecular assembly of surfactants as structure-directing agents have attracted interest in applications where solid/gas and solid/liquid interface plays an important role, in particular, catalysis and electrochemistry [3–11]. Precise control in the pore structure, such as pore size, wall thickness, and pore connection, of such ordered mesoporous materials should allow high rates of mass transport, an essential aspect for many applications. Well-ordered porous metals including Pt, Ni, etc. have so far been reported. The utilization of soft-templates allow fine-tuning of ordered pores with size in the mesoporous regime, the dimensions depending on the size of the organic template used and other synthetic parameters. A distinctive characteristic of the synthesis of ordered mesoporous metals in contrast to other ordered mesoporous materials such as oxides and carbon is that the reduction process is conducted under mild conditions, i.e. near-room temperature, which allows preservation of the ordered structure. This is clearly a different methodology compared to the synthesis of ordered mesoporous oxides and carbon, where post-heat treatment is typically applied to convert the polymeric precursor to a rigid structure. In the case of ordered mesoporous metals, the metal precursor is converted directly to crystalline nanoparticles by chemical or electrochemical methods, thereby forming a rigid framework that can withstand template removal. Direct deposition of oxides is not as straightforward as metals, as chemical oxidation or polarization to cathodic potentials lead to collapse of the mesoporous framework. Formation of nickel hydroxide surface layers on ordered mesoporous nickel (NiOOH/Ni) by electrochemical oxidation methods has been reported [12–17]. Such an approach should be useful in preparing oxides with a mesoporous framework without the need of post-heat treatment.

* Corresponding author at: Faculty of Textile Science and Technology, Shinshu University, 3-15-1 Tokida, Ueda, Nagano 386-8567, Japan. Tel.: +81 268 21 5455; fax: +81 268 21 5452.
** Corresponding author at: World Premier International Research Center for Materials Nanoarchitectonics, National Institute for Materials Science, Namiki 1-1, Tsukuba, Ibaraki 305-0044, Japan. Tel.: +81 29 860 4635.
E-mail addresses: wsugi@shinshu-u.ac.jp (W. Sugimoto), Yamauchi.Yusuke@nims.go.jp (Y. Yamauchi).
[1] Present address: Office of Society-Academia Collaboration for Innovation, Kyoto University, 1-1-1 Koutou, Sayo-cho, Sayo-gun, Hyogo 679-5198, Japan.
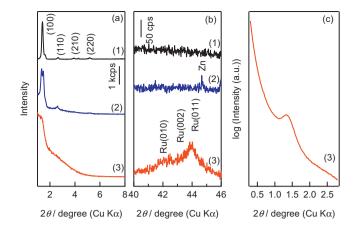
In this study, we focused on the synthesis of ordered mesoporous Ru and its conversion to RuO_x. Ruthenium nanoparticles find applications in many catalytic applications [18–22]. Commercially available high-surface area Ru black has typical average particle size of c.a. 10 nm and specific surface area of <50 $m^2 g^{-1}$. Takai et al. have briefly reported on the synthesis of mesoporous Ru black with surface area of 62 $m^2 g^{-1}$ via lyotropic crystal templating as the end member of the Pt–Ru alloy [23]. In addition to metallic Ru, high surface area ruthenium oxide is also an important material for various applications, including electrocatalysts for chlorine evolution [24], electrochemical capacitor electrodes [25–29], as well as fuel cell electrocatalysts [30–39]. The small particle size (1–2 nm) and the existence of appreciable pores are important requirements for the high capacitance [40–42]. The synthesis of high capacitance RuO_2 (~700 $F g^{-1}$) have been conducted mainly by sol–gel synthesis, leading to materials with random micropores [25,26]. Surfactant assisted synthesis of ordered mesoporous RuO_2 have so far lead to material with substantially low capacitance values, i.e. 100 $F g^{-1}$ [43,44], which is likely due to particle ripening and pore collapse due to post heat treatment. Two studies have succeeded in the synthesis of high capacitance mesoporous RuO_2, albeit with poorly or no ordered structures [45,46]. Here we report the synthesis and detailed structural and electrochemical characterization of metallic Ru using a non-ionic surfactant as the structure directing agent. Furthermore, we demonstrate for the first time, the conversion of ordered mesoporous Ru to RuO_x possessing a well-ordered mesoporous structure by electro-oxidation.

2. Experimental

A non-ionic surfactant, Brij56 ($C_{16}H_{33}(OCH_2CH_2)_nOH$, $n\sim10$) was added into aqueous $RuCl_3 \cdot nH_2O$ in the desired ratios (Brij56:$RuCl_3 \cdot nH_2O$:H_2O = 3:8:8 in mass) to obtain a hexagonal lyotropic liquid crystal with Ru^{n+} in the aqueous domain. Zn (sandy Zn; 1–4 mm) was then added in appropriate amounts and aged for 1 week at 15 °C to reduce ruthenium ions. The product was thoroughly washed with ethanol to remove the surfactant. Residual Zn was removed by acid treatment with 5 M H_2SO_4. The structure of the products was characterized by X-ray diffraction [XRD, Rigaku RINT-2550 with monochromated CuKα radiation], small-angle X-ray scattering [SAXS, Rigaku Nano-Viewer with monochromated CuKα radiation], transmission electron microscopy [HRTEM, JEOL JEM-2010] and high-resolution scanning electron microscopy [HRSEM, Hitachi S-5000].

A beaker-type electrochemical cell equipped with the working electrode, a platinum mesh counter electrode and a Ag/AgCl/KCl (sat.) reference electrode connected with a salt bridge was used. A Luggin capillary faced the working electrode at a distance of 2 mm. All electrode potentials throughout the paper will be referred to the reversible hydrogen electrode (RHE) scale. Ordered mesoporous Ru (20 mg) was dispersed in ultrapure water (>18 MΩ cm) (10 mL) and 20 μL of the dispersion was casted onto a glassy carbon electrode (5 mm in diameter) with a micro-pipette. A 5 wt% Nafion solution (20 μL) was dropped onto the electrode to affix the powder onto the current collector and dried. Electro-oxidation of pre-adsorbed carbon monoxide (CO_{ad}) was measured by CO_{ad} stripping voltammetry in 0.5 M H_2SO_4 at a scan rate of 10 mV s^{-1}. Gaseous CO was purged into the electrolyte for 40 min to allow complete adsorption of CO onto the catalyst surface while maintaining a constant voltage of 50 mV. Excess CO in the electrolyte was then purged out by bubbling N_2 gas for 40 min. The electrochemical surface area of Ru was calculated from the CO stripping voltammograms. The amount of CO_{ad} was estimated by integration of the CO_{ad} stripping peak, corrected for the electrical double-layer capacitance, assuming a monolayer of linearly adsorbed CO

Fig. 1. (a, b) XRD and (c) SAXS patterns of (1) Ru^{n+}–LLC mixture before reduction, (2) after Zn reduction of (1), and (3) after template and Zn removal of (2).

on the Ru surface and the Coulombic charge necessary for oxidation as 420 μC cm^{-2}. Electrochemical oxidation was conducted by potential cycling between 0.2 and 1.2 V vs. RHE at 50 mV s^{-1} for 500 cycles. The pseduo-capacitance of the electro-oxidized sample was calculated by averaging the anodic and cathodic charge. Comparative experiments with unsupported Ru black (kindly provided by N.E. Chemcat Co.) and carbon supported Ru (Ru/C; 30 mass% Ru on Vulcan Carbon prepared by an impregnation method [47].

3. Results and discussion

The XRD patterns of the complex of surfactant (Brij 56) and Ru precursor ($RuCl_3 \cdot nH_2O$) can be indexed based on a hexagonal symmetry indicating the successful preparation of a hexagonal lyotropic liquid crystalline (LLC) phase (Fig. 1a). Successful reduction of ruthenium ions to metallic Ru with Zn is evidenced by the development of weak diffraction peaks which can be indexed as the (0 1 0), (0 0 2) and (0 1 1) planes of hcp Ru (Fig. 1b). Evidence of mesoscale ordering is still evident after removal of surfactant and residual Zn, though the low angle diffraction peaks are broadened. SAXS provided clear evidence of the preservation of the mesoscale ordering after reduction and surfactant removal with d = 6.4 nm (Fig. 1c). Electron microscopy studies furnished direct imaging of ordered mesopores after the surfactant removal. Spherical particles of about 50 nm in diameter are observed by SEM (Fig. 2a). The surface of the particles is severely rough, suggesting a porous nanostructure. A TEM image is shown in Fig. 2b, which shows that each particle is constituted by hexagonally arranged arrays of pores with pore to pore distance of 5.7 nm. High resolution images shows that the walls are constituted by crystalline Ru particles with diameter of about 2–3 nm. It is also noted that the SEM image reveals that the ordered mesostructure is observed over a wide range in the micrometer scale (Fig. 2).

The mesoporous Ru obtained in this study seems to be slightly less homogeneous compared to reported mesoporous Pt analogue prepared by similar procedures, which is consistent with the study of ordered mesoporous Pt–Ru alloys where the degree of ordering was found to decrease with the increase in Ru content [23]. Although a straightforward comparison may be difficult based on the different synthetic conditions, the difference in nucleation energy of the metals may play an important factor. Pt is fairly stable in a nanoparticle form, whereas Ru is known to easily aggregate into larger particles [47].

The electrochemically active surface area of ordered mesoporous Ru metal was measured by the CO-stripping method (Fig. 3). Two control samples with similar geometry were also
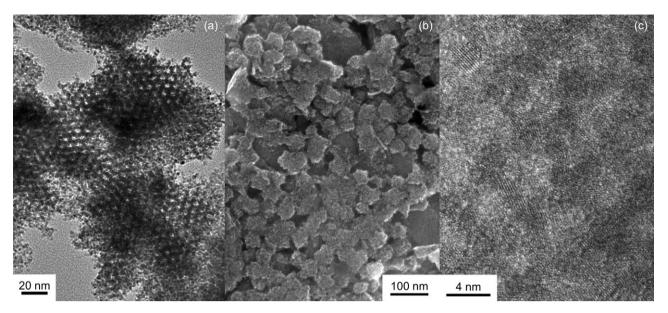
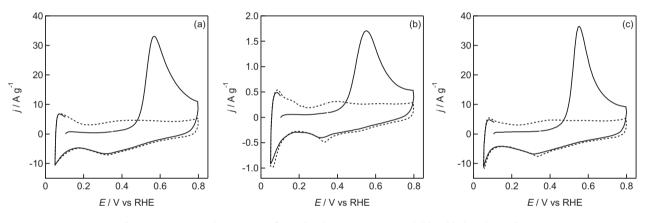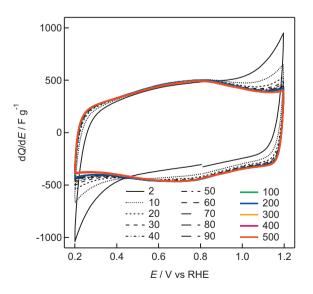**Fig. 2.** (a, c) TEM and (b) SEM images of mesoporous Ru.

Fig. 3. CO-stripping voltammogram of (a) ordered mesoporous Ru metal, (b) Ru black, and (c) Ru/C.

characterized; namely, Ru black with particle size of ∼50 nm, and Ru nanoparticles with diameter of ∼3 nm supported on carbon (Fig. S1). The feature of the voltammogram of ordered mesoporous Ru metal (Fig. 3a) closely matches that of Ru black (Fig. 3b) and Ru/C (Fig. 3c). The specific surface area of ordered mesoporous Ru metal is 110 m^2 g^{-1}; considerably larger than the value for Ru black (6 m^2 g^{-1}) and comparable to carbon supported Ru nanoparticles (100 m^2 g^{-1}). This large surface area is a consequence of the characteristic mesoporous structure.

Electrochemical oxidation of the ordered mesoporous Ru metal was conducted by sweeping the potential between 0.2 and 1.2 V vs. RHE at 25 °C for 500 cycles at 50 mV s^{-1} (Fig. 4). In the initial cycles, oxidation currents around 1.0–1.2 V and reduction current near 0.2–0.4 V and can be observed, with the oxidation–reduction currents decreasing with consecutive cycling. The anodic charge is larger than the cathodic charge, and is equalized after 100 cycles. These are attributed to surface oxidation and slow surface reduction [48]. The number of cycles necessary to obtain steady-state is similar to the case of Ru/C and Ru black (Fig. S2), suggesting that the kinetics of the electro-oxidation process of ordered mesoporous Ru is similar to Ru/C and Ru black. It should be noted that the capacitance of electro-oxidized Ru black at 2 mV s^{-1} was 17 F (g-Ru)$^{-1}$ after 100 cycles and does not increase with consecutive cycling.

Fig. 4. Cyclic voltammograms of the first 500 cycles during the electro-oxidation process of ordered mesoporous Ru metal.
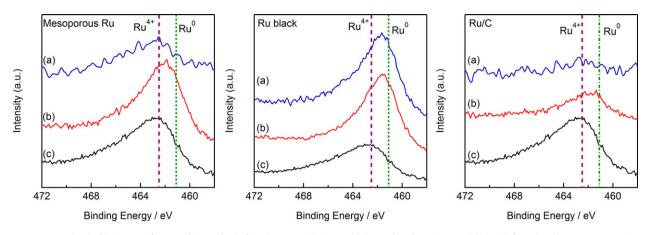
Fig. 5. XPS Ru3p core-level of (a) RuO$_2$ reference, (b) samples before electro-oxidation, and (c) samples after electro-oxidation (left) ordered mesoporous Ru, (center) Ru black, and (right) Ru/C.
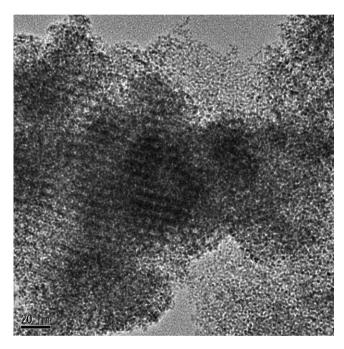

Fig. 6. TEM image of ordered mesoporous RuO$_x$, the electro-oxidized product of ordered mesoporous Ru.

Under the present conditions, only the surface and/or near surface layers may have been oxidized.

The redox peaks in the hydrogen adsorption/desorption (0.05–0.2 V vs. RHE) and surface oxide reduction (0.3 V vs. RHE) peaks characteristic of metallic Ru (Fig. 3a) are no longer observed after electro-oxidation (Fig. 4). The voltammogram after electro-oxidation has the typical featureless shape of an ideally polarizable electrode with some contribution from surface redox processes at 0.7 V vs RHE. CO-stripping voltammetry was conducted on the electro-oxidized sample to confirm the irreversible oxidation of Ru to RuO$_x$. No CO oxidation current could be detected after electro-oxidation, confirming the absence of metallic Ru on the surface. Oxidation of Ru was also supported by XPS, revealing a shift in the Ru3p and Ru3d peaks to higher binding energy (Fig. 5). Fig. 6 shows a typical TEM image of the product after electro-oxidation. Clearly, the ordered mesoporous structure is preserved after electro-oxidation.

The specific capacitance of the ordered mesoporous RuO$_x$ was 376 F (g-RuO$_2$)$^{-1}$, closely matching the value of 350 F g^{-1} reported for RuO$_x$ obtained by electro-oxidation of a Ru film [49]. This is the highest reported value for RuO$_x$ material with a well-ordered mesoporous structure. The major difference with other methods that have employed templates is that the present procedure does not involve any heat treatment to remove the template. Such treatment would results in pore collapse, particle ripening, and loss of intra-particle water, in turn leading to smaller surface area and specific capacitance [43,44]. The specific capacitance is unfortunately smaller than reported values for RuO$_2 \cdot n$H$_2$O prepared by sol–gel synthesis [25,26], most likely due to the larger primary particle size of RuO$_x$ (2–3 nm in diameter) constituting the walls and possible incomplete oxidation.

4. Conclusion

We have successfully prepared ruthenium oxide with a well-ordered mesoporous structure with specific capacitance of 376 F g^{-1}. The use of lyotropic liquid crystals as soft templates was utilized to first prepare metallic ruthenium. Various characterization techniques clearly indicated that the obtained ruthenium black was composed of well-ordered mesopores in a hexagonal array with electrochemically active surface area of 110 m^2 g^{-1}. Subsequent electro-oxidation afforded the oxidized analogue; i.e. ordered mesoporous ruthenium oxide, applicable to supercapacitor applications. The present synthetic approach is anticipated to explicate a general process for the synthesis of oxides with ordered nanostructures.

Acknowledgment

Appendix A. Supplementary data

Supplementary data associated with this article can be found, in the online version, at doi:10.1016/j.jpowsour.2011.12.033.

References

[1] G.S. Attard, P.N. Bartlett, N.R.B. Coleman, J.M. Elliott, J.R. Owen, J.H. Wang, Science 278 (1997) 838–840.
[2] G.S. Attard, C.G. Göltner, J.M. Corker, S. Henke, R.H. Templer, Angew. Chem. Int. Ed. Engl. 36 (1997) 1315–1317.
[3] F. Schüth, Chem. Mater. 13 (2001) 3184–3195.
[4] C. Rao, D. Trivedi, Coord. Chem. Rev. 249 (2005) 613–631.
[5] F. Bender, R.K. Mankelow, D.B. Hibbert, J.J. Gooding, Electroanalysis 18 (2006) 1558–1563.
[6] B. Smarsly, M. Antonietti, Eur. J. Inorg. Chem. 2006 (2006) 1111–1119.

[7] M.G. Kanatzidis, Adv. Mater. 19 (2007) 1165–1181.
[8] Y. Yamauchi, K. Kuroda, Chem. Asian J. 3 (2008) 664–676.
[9] C. Wang, D. Chen, X. Jiao, Sci. Tech. Adv. Mater. 10 (2009) 023001.
[10] Y. Yamauchi, N. Suzuki, L. Radhakrishnan, L. Wang, Chem. Rec. 9 (2009) 321–339.
[11] A. Walcarius, Anal. Bioanal. Chem. 396 (2010) 261–272.
[12] P.A. Nelson, J.M. Elliott, G.S. Attard, J.R. Owen, Chem. Mater. 14 (2002) 524–529.
[13] P.A. Nelson, J.R. Owen, J. Electrochem. Soc. 150 (2003) A1313–A1317.
[14] V. Ganesh, V. Lakshminarayanan, Electrochim. Acta 49 (2004) 3561–3572.
[15] V. Ganesh, V. Lakshminarayanan, S. Pitchumani, Electrochem. Solid-State Lett. 8 (2005) A308.
[16] D. Zhao, S. Bao, W. Zhou, H. Li, Electrochem. Commun. 9 (2007) 869–874.
[17] D. Zhao, W. Zhou, H. Li, Chem. Mater. 19 (2007) 3882–3891.
[18] A.S. Aricò, S. Srinivasan, V. Antonucci, Fuel Cells 1 (2001) 133–161.
[19] J.-W. Lee, B.N. Popov, J. Solid State Electrochem. 11 (2007) 1355–1364.
[20] F. Lu, J. Liu, J. Xu, Mater. Chem. Phys. 108 (2008) 369–374.
[21] A. Nowicki, Y. Zhang, B. Léger, J.-P. Rolland, H. Bricout, E. Monflier, A. Roucoux, Chem. Commun. (2006) 296–298.
[22] J. Ning, J. Xu, J. Liu, F. Lu, Catal. Lett. 109 (2006) 175–180.
[23] A. Takai, T. Saida, W. Sugimoto, L. Wang, Y. Yamauchi, K. Kuroda, Chem. Mater. 21 (2009) 3414–3423.
[24] S. Trasatti, Electrochim. Acta 36 (1991) 225–241.
[25] J.P. Zheng, P.J. Cygan, T.R. Jow, J. Electrochem. Soc. 142 (1995) 2699–2703.
[26] J.P. Zheng, T.R. Jow, J. Electrochem. Soc. 142 (1995) L6–L8.
[27] W. Sugimoto, K. Yokoshima, Y. Murakami, Y. Takasu, Electrochim. Acta 52 (2006) 1742–1748.
[28] K. Fukuda, T. Saida, J. Sato, M. Yonezawa, Y. Takasu, W. Sugimoto, Inorg. Chem. 49 (2010) 4391–4393.
[29] W. Sugimoto, H. Iwata, Y. Yasunaga, Y. Murakami, Y. Takasu, Angew. Chem. Int. Ed. Engl. 42 (2003) 4092–4096.
[30] J.W. Long, R.M. Stroud, K.E. Swider-Lyons, D.R. Rolison, J. Phys. Chem. B 104 (2000) 9772–9776.
[31] D.R. Rolison, P.L. Hagans, K.E. Swider, J.W. Long, Langmuir 15 (1999) 774–779.
[32] H.M. Villullas, F.I. Mattos-Costa, L.O.S. Bulhões, J. Phys. Chem. B 108 (2004) 12898–12903.
[33] B.J. Kennedy, A.W. Smith, J. Electroanal. Chem. 293 (1990) 103–110.
[34] L. Cao, F. Scheiba, C. Roth, F. Schweiger, C. Cremers, U. Stimming, H. Fuess, L. Chen, W. Zhu, X. Qiu, Angew. Chem. Int. Ed. Engl. 45 (2006) 5315–5319.
[35] Z. Chen, X. Qiu, B. Lu, S. Zhang, W. Zhu, L. Chen, Electrochem. Commun. 7 (2005) 593–596.
[36] W. Sugimoto, T. Saida, Y. Takasu, Electrochem. Commun. 8 (2006) 411–415.
[37] T. Saida, W. Sugimoto, Y. Takasu, Electrochim. Acta 55 (2010) 857–864.
[38] F. Peng, C. Zhou, H. Wang, H. Yu, J. Liang, J. Yang, Catal. Commun. 10 (2009) 533–537.
[39] C. Bock, A. Collier, B. MacDougall, J. Electrochem. Soc. 152 (2005) A2291–A2299.
[40] D.A. McKeown, P.L. Hagans, L.P.L. Carette, A.E. Russell, K.E. Swider, D.R. Rolison, J. Phys. Chem. B 103 (1999) 4825–4832.
[41] W. Dmowski, T. Egami, K.E. Swider-Lyons, C.T. Love, D.R. Rolison, J. Phys. Chem. B 106 (2002) 12677–12683.
[42] W. Sugimoto, H. Iwata, K. Yokoshima, Y. Murakami, Y. Takasu, J. Phys. Chem. B 109 (2005) 7330–7338.
[43] K.-M. Lin, K.-H. Chang, C.-C. Hu, Y.-Y. Li, Electrochim. Acta 54 (2009) 4574–4581.
[44] V. Subramanian, S.C. Hall, P.H. Smith, B. Rambabu, Solid State Ionics 175 (2004) 511–515.
[45] S.H. Oh, L.F. Nazar, J. Mater. Chem. 20 (2010) 3834–3839.
[46] C. Sassoye, C. Laberty, H. Le Khanh, S. Cassaignon, C. Boissière, M. Antonietti, C. Sanchez, Adv. Funct. Mater. 19 (2009) 1922–1929.
[47] T. Kawaguchi, W. Sugimoto, Y. Murakami, Y. Takasu, J. Catal. 229 (2005) 176–184.
[48] S. Hadži-Jordanov, H. Angerstein-Kozlowska, B.E. Conway, J. Electroanal. Chem. Interfacial Electrochem. 60 (1975) 359–362.
[49] I.D. Raistrick, R.T. Sherman, in: H.W.S. Srinivasan, S. Wagner (Eds.), The Electrochemical Society Proceedings Series PV 87-12 Electrode Materials and Processes for Energy Conversion and Storage, The Electrochemical Society, Pennington, NJ, 1987, p. 582.